12-5 REACTANCE TRANSFORMATIONS AND MOEBIUS MAPPINGS

All filter types described thus far represent approximations to the ideal low-pass brick-wall response shown in Fig. 12-3. With a simple manipulation, however, all previous results can be applied to a variety of other problems. Assume, for example, that in the filter of Fig. 12-17*a* the inductor L_2 is replaced by a capacitor C'_2 and, vice versa, all capacitors C_1, C_2, C_3 are replaced by inductors L'_1, L'_2, L'_3, respectively (Fig. 12-19*a*). Assume furthermore that the new element values satisfy the relations

$$C'_2 = \frac{1}{AL_2} \qquad L'_i = \frac{1}{AC_i} \qquad i = 1, 2, 3 \tag{12-89}$$

What will the response of this new filter be?

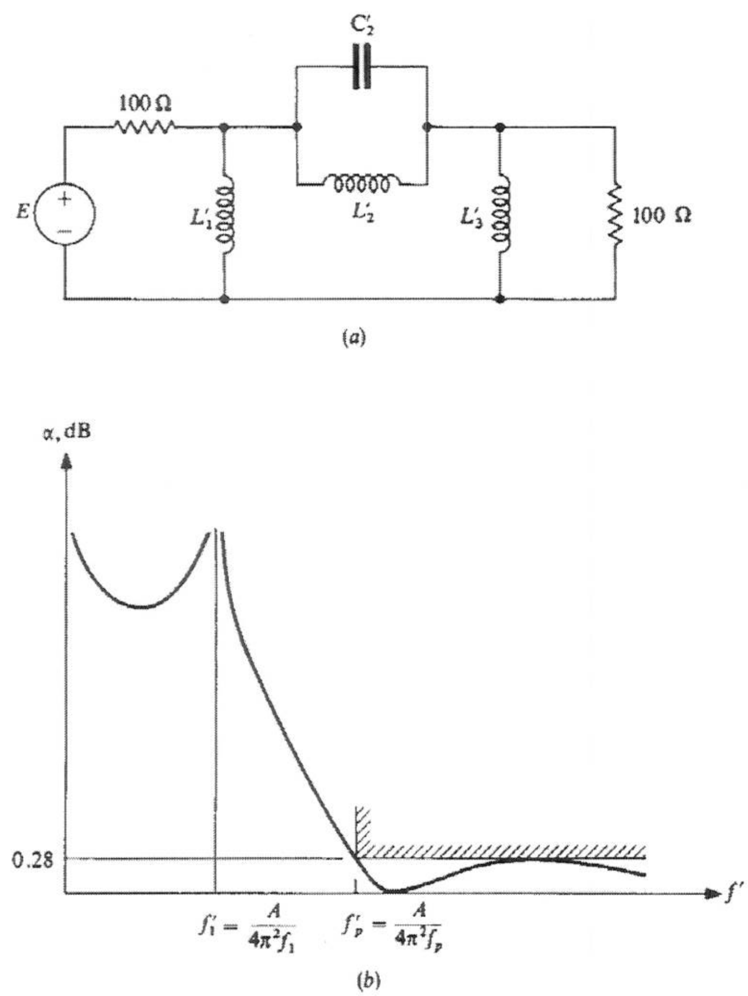

Figure 12-19 (*a*) High-pass filter obtained by transforming the filter of Fig. 12-17*a*; (*b*) loss response.

In the calculation of the original filter response, ω enters only through the reactive immittances $j\omega L_2$, $j\omega C_1$, $j\omega C_2$, and $j\omega C_3$. In the new filter, these immitances are replaced, according to Fig. 12-19*a* and Eq. (12-89), as follows:

$$j\omega L_i \rightarrow \frac{1}{j\omega' C'_i} = \frac{-jAL_i}{\omega'} \qquad i = 2$$
$$j\omega C_i \rightarrow \frac{1}{j\omega' L'_i} = \frac{-jAC_i}{\omega'} \qquad i = 1, 2, 3 \tag{12-90}$$

where ω' is the radian frequency variable of the new filter. Hence, in effect, the variable ω has been replaced by the new variable ω' through the relation

$$\omega = -\frac{A}{\omega'} \tag{12-91}$$

For example, $A = 2 \times 10^8$. Then the loss value 0.28 dB, which the original filter had at its passband limit $f_p = 10$ kHz (Fig. 12-17), will be obtained for the new filter at

$$\omega' = -\frac{A}{\omega_p} = -\frac{2 \times 10^8}{2\pi 10^4} = -\frac{10^4}{\pi}\text{ rad/s} \tag{12-92}$$

or

$$f' = -\frac{10^4}{2\pi^2} \approx -0.5066 \text{ kHz} \tag{12-93}$$

Since the loss response is an even function of f', the loss will be the same at $f'_p \triangleq +0.5066$ kHz. Equation (12-91) also shows that loss values in the original passband $|f| \leq f_p$ will appear in the range $|f'| \geq f'_p$ for the new filter (Fig. 12-19*b*), and vice versa. Thus, the filter obtained through the transformation described by Eqs. (12-90) and (12-91) from a low-pass filter is a *high-pass filter*. The frequency values related by the transformation (12-91) can be easily visualized if we plot the ω-vs.-ω' curve (Fig. 12-20*a*). Figure 12-20*b* illustrates schematically† the change in the loss response due to the transformation.

Assume now that a high-pass filter with specified values of ω'_p, ω'_s, α_p, and α_s must be designed. The techniques of Secs. 12-2 to 12-4 enable us to design a *low-pass* filter from which the final high-pass circuit is obtainable using (12-90) and (12-91). Hence, we need merely to find the parameters ω_p, ω_s of the low-pass filter and the transformation constant A. The selectivity parameter k of the low-pass filter satisfies, by (12-91),

$$k \triangleq \frac{\omega_p}{\omega_s} = \frac{-A/\omega'_p}{-A/\omega'_s} = \frac{\omega'_s}{\omega'_p} \tag{12-94}$$

and is thus known. When ω_p is chosen arbitrarily (say at $\omega_p = 1$), the transformation constant A is given, from (12-92), by

$$A = \omega_p \omega'_p \tag{12-95}$$

† For a Chebyshev filter.

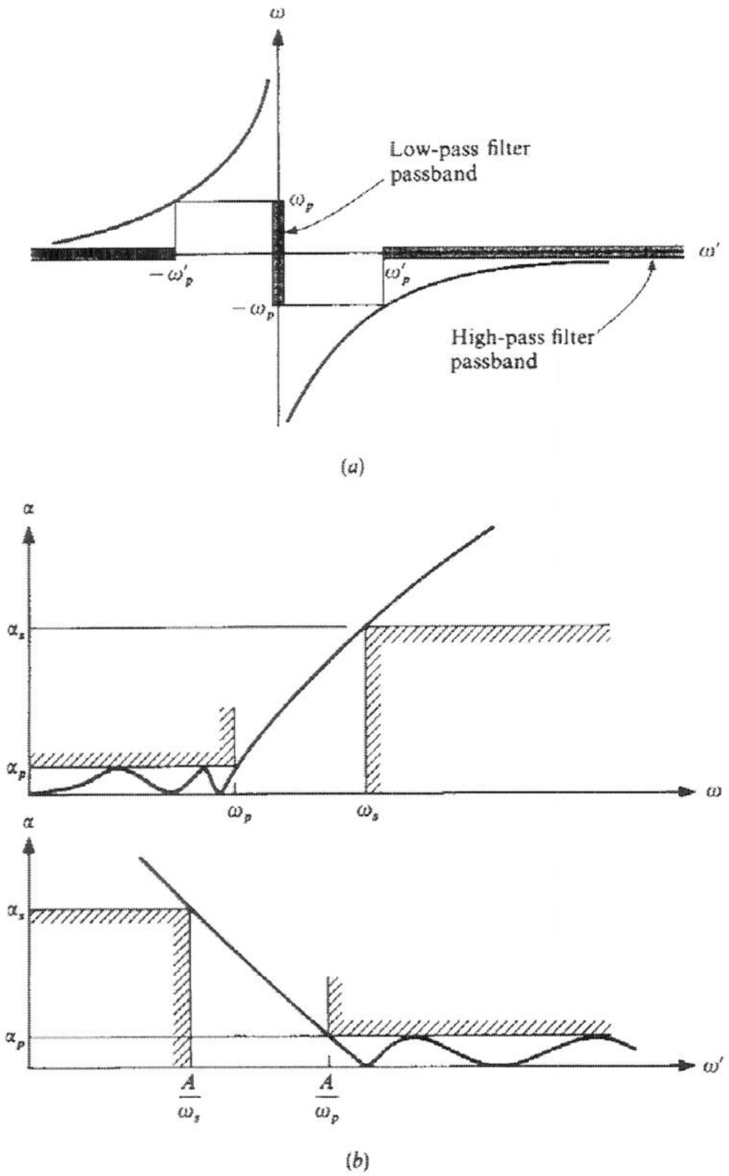

Figure 12-20 (*a*) Relation between the low-pass and high-pass frequency variables; (*b*) the resulting transformation of the loss response.

We conclude that the high-pass filter design using a low-pass prototype filter can be carried out in the following steps:

1. From the specified high-pass filter parameters α_p, α_s, f'_p, f'_s, the selectivity $k = f'_s/f'_p < 1$ of the low-pass prototype is found, and ω_p is chosen.
2. From ω_p, $\omega_s = \omega_p/k$, α_p, and α_s, the low-pass filter is designed.†

† Note that α_p and α_s remain the same for the low-pass and high-pass filters since our transformation affects only the ω axis.

3. From the elements of the low-pass filter, those of the desired high-pass filter can be obtained using the relations

$$C'_i = \frac{1}{AL_i} = \frac{1}{\omega_p \omega'_p L_i} \qquad i = 1, 2, \ldots$$
$$L'_i = \frac{1}{AC_i} = \frac{1}{\omega_p \omega'_p C_i} \qquad i = 1, 2, \ldots \tag{12-96}$$

Example 12-6 Design a high-pass filter satisfying the following specifications:

$$\alpha \leq 0.1 \text{ dB} \qquad \text{for } f \geq 15 \text{ kHz}$$
$$\alpha \geq 40 \text{ dB} \qquad \text{for } f \leq 2.5 \text{ kHz}$$

Terminating resistors: 600 Ω

Following the design steps outlined above, we find for the low-pass prototype filter the selectivity parameter

$$k = \frac{\omega_p}{\omega_s} = \frac{f'_s}{f'_p} = \frac{2.5 \times 10^3}{15 \times 10^3} = \frac{1}{6}$$

and, from (12-24), the discrimination parameter

$$k_1 = \sqrt{\frac{10^{\alpha_p/10} - 1}{10^{\alpha_s/10} - 1}} \approx 1.52628 \times 10^{-3}$$

Hence, choosing a Chebyshev filter, by (12-71) the degree must satisfy

$$n \geq \frac{\cosh^{-1}(1/k_1)}{\cosh^{-1}(1/k)} \approx 2.896$$

Using $n = 3$ and postulating (for a change)

$$\alpha(f_p) = \alpha_p \qquad \alpha(f_s) > \alpha_s$$

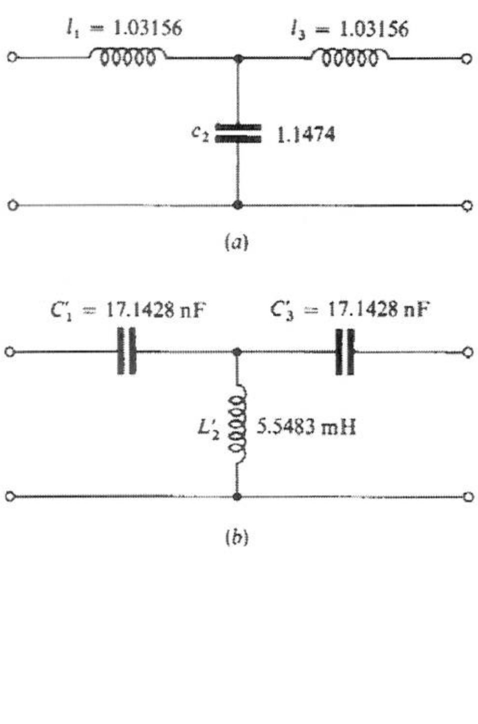

Figure 12-21 (*a*) Normalized low-pass prototype filter; (*b*) final high-pass filter circuit.

we get an increased stopband loss of 42.218 dB. Proceeding with the calculation of $K(S)$, $H(S)$, and the element values, as discussed in Sec. 12-3, we obtain the circuit shown in Fig. 12-21a. This circuit is both frequency- and impedance-normalized: it is designed with $\omega_p = 1$ and $R_G = R_L = 1$.

Next, the circuit is transformed, element by element, into an impedance-normalized high-pass filter. Using (12-95), we obtain

$$A = \omega_p \omega'_p = (1)(2\pi)(15 \times 10^3) \approx 9.424778 \times 10^4$$

and hence, by (12-96),

$$c'_1 = c'_3 = \frac{1}{Al_1} \approx 1.02857 \times 10^{-5} \qquad \text{and} \qquad l'_2 = \frac{1}{Ac_2} = 0.924728 \times 10^{-5}$$

Finally, impedance denormalization is accomplished by multiplying l'_2 by 600 and dividing c'_1 as well as c'_3 by 600. This gives the final circuit shown in Fig. 12-21b.

It is clear that the transformation $\omega = -A/\omega'$ given in (12-91) performs two functions: (1) it replaces a low-pass frequency response by a high-pass one; (2) it replaces the element immittances in the low-pass prototype by realizable immittances in the high-pass circuit, as Eqs. (12-89) and (12-90) illustrate. Next, consider the transformation

$$\omega = -A\frac{\omega_1^2 - \omega'^2}{\omega'} \qquad (12\text{-}97)$$

This replaces an inductance in the prototype network by an impedance according to the relation

$$j\omega L_i = -jA\frac{\omega_1^2 L_i}{\omega'} + jAL_i\omega' = \frac{1}{j\omega' C'_i} + jL'_i\omega' \qquad (12\text{-}98)$$

where

$$C'_i \triangleq \frac{1}{A\omega_1^2 L_i} \qquad L'_i \triangleq AL_i \qquad (12\text{-}99)$$

Clearly, L_i becomes a series resonant circuit (Fig. 12-22a) in the transformed network. The resonant frequency is

$$\omega_r = \frac{1}{\sqrt{L'_i C'_i}} = \omega_1 \qquad (12\text{-}100)$$

Similarly, a capacitor is replaced as suggested by

$$j\omega C_i = -jA\frac{\omega_1^2 C_i}{\omega'} + jAC_i\omega' = \frac{1}{j\omega' L'_i} + j\omega' C'_i \qquad (12\text{-}101)$$

The capacitor C_i is thus transformed into a parallel resonant circuit (Fig. 12-22b). The element values are, from (12-101),

$$L'_i \triangleq \frac{1}{A\omega_1^2 C_i} \qquad C'_i \triangleq AC_i \qquad (12\text{-}102)$$

The resonant frequency is again given by (12-100).

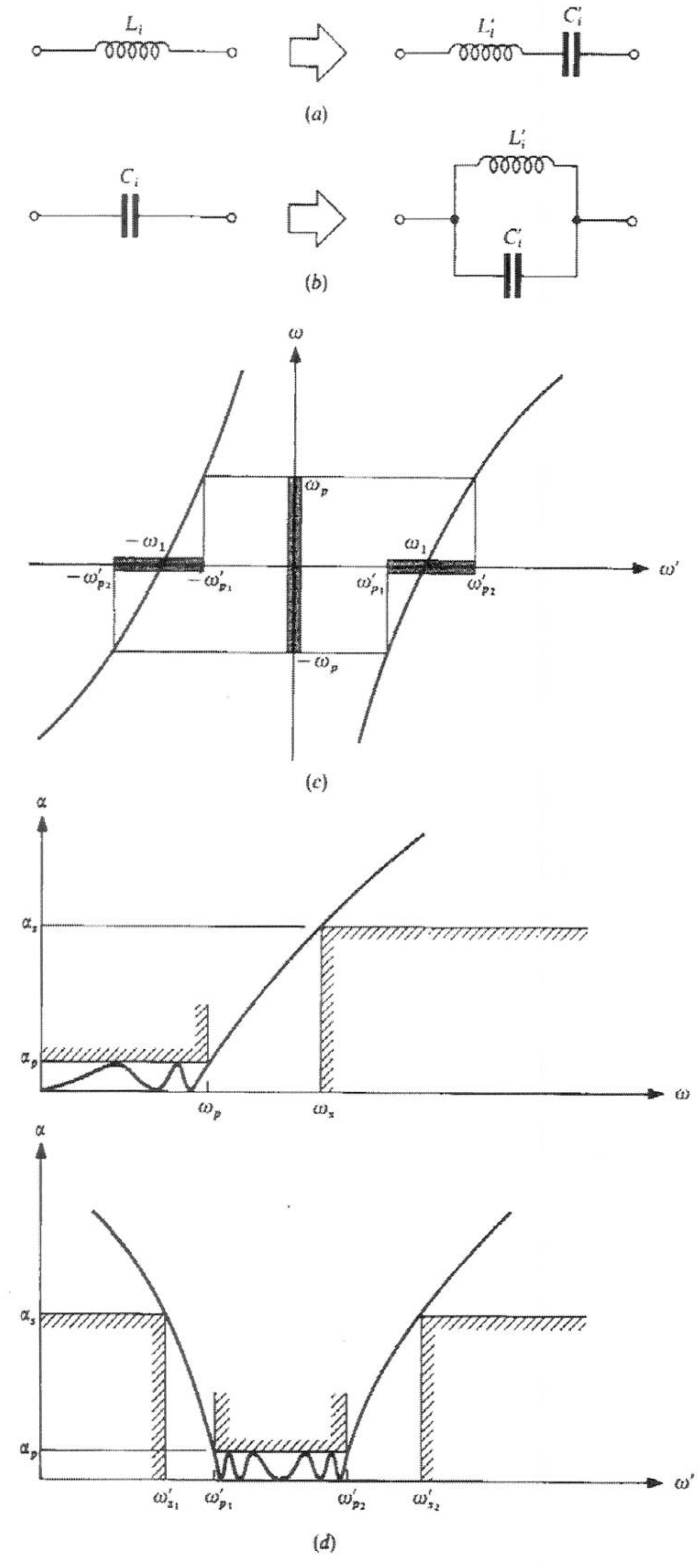

Figure 12-22 (*a*) and (*b*). The transformation of low-pass prototype elements into bandpass filter impedances; (*c*) the corresponding transformation of the frequency variable; (*d*) the effect of the transformation on the loss response.

To find the effect of the transformation (12-97) on the frequency response, the ω-vs.-ω' curve can be plotted. The result (Fig. 12-22*c*) demonstrates that now the frequency range $-\omega_p \le \omega \le \omega_p$ is transformed into the ranges $-\omega'_{p2} \le \omega' \le -\omega'_{p1}$ and $\omega'_{p1} \le \omega' \le \omega'_{p2}$. Hence, if the prototype circuit was a low-pass filter, the transformed circuit will be a *bandpass* one. Figure 12-22*d* illustrates the bandpass-filter response obtained. The passband limits ω'_{p1} and ω'_{p2} can be obtained from (12-97). As Fig. 12-22*c* shows, ω_p transforms into $-\omega'_{p1}$ and ω'_{p2}; hence, the latter frequencies are the solutions of the equation

$$\omega_p = -A\frac{\omega_1^2 - \omega'^2}{\omega'} \qquad \omega'^2 - \frac{\omega_p}{A}\omega' - \omega_1^2 = 0 \tag{12-103}$$

ω : low-pass

ω' : high-pass

$\omega = \dfrac{-A}{\omega'}$

Hence, ω'_{p1} and ω'_{p2} satisfy the relations

$$\begin{gathered}(\omega' + \omega'_{p1})(\omega' - \omega'_{p2}) = \omega'^2 - \frac{\omega_p}{A}\omega' - \omega_1^2 \\ \omega'_{p2} - \omega'_{p1} = \frac{\omega_p}{A} \qquad \omega'_{p1}\omega'_{p2} = \omega_1^2\end{gathered} \tag{12-104}$$

In the same way, the stopband limit ω_s of the low-pass filter transforms into the high-pass filter stopband limit frequencies $-\omega'_{s1}$ and ω'_{s2}. Performing an analysis exactly analogous to that giving (12-104) gives the results

$$\omega'_{s2} - \omega'_{s1} = \frac{\omega_s}{A} \qquad \omega'_{s1}\omega'_{s2} = \omega_1^2 \tag{12-105}$$

As Eqs. (12-104) and (12-105) show, if the low-pass filter has a loss α at frequency ω, the same loss will be obtained for the bandpass filter at the positive frequencies ω'_a and ω'_b; these frequencies will have a geometric symmetry around ω_1 so that $\omega'_a\omega'_b = \omega_1^2$. Hence, the loss response of the bandpass filter will have a geometric symmetry around ω_1.

At this stage, we can piece together the design procedure for a bandpass filter using a low-pass prototype. The design steps are the following:

1. We check the given bandpass-filter parameters ω'_{p1}, ω'_{p2}, ω'_{s1}, and ω'_{s2} to see whether the geometric symmetry condition

$$\omega'_{p1}\omega'_{p2} = \omega'_{s1}\omega'_{s2} \tag{12-106}$$

[which follows from Eqs. (12-104) and (12-105)] is met. If not, one of the parameters can be readjusted to restore symmetry *and* introduce some safety margin. If, for example,

$$\omega'_{p1}\omega'_{p2} > \omega'_{s1}\omega'_{s2} \tag{12-107}$$

then ω'_{p1} can be lowered to $\omega'_{s1}\omega'_{s2}/\omega'_{p2}$.

2. The selectivity of the low-pass filter prototype can be found from (12-104) and (12-105):

$$k \triangleq \frac{\omega_p}{\omega_s} = \frac{A(\omega'_{p2} - \omega'_{p1})}{A(\omega'_{s2} - \omega'_{s1})} = \frac{\omega'_{p2} - \omega'_{p1}}{\omega'_{s2} - \omega'_{s1}} \tag{12-108}$$

From k, α_p, and α_s, the low-pass prototype filter can be designed. Since in the design process the degree n is rounded *up*, k will actually be higher than the value given by (12-108).

3. To obtain the element values of the bandpass filter from those of the prototype, the transformation constants A and ω_1^2 are needed. They in turn can be obtained from the limit frequencies of the filters. From (12-108) and (12-106)

$$\omega'_{p2} - \omega'_{p1} = k(\omega'_{s2} - \omega'_{s1}) \qquad \omega'_{p2}\omega'_{p1} = \omega'_{s2}\omega'_{s1} \tag{12-109}$$

where k is the actual (increased) selectivity of the low-pass filter. Keeping, say, ω'_{s1} and ω'_{s2} at their specified values, we obtain a second-degree equation

$$(\omega'_{p2})^2 - k(\omega'_{s2} - \omega'_{s1})\omega'_{p2} - \omega'_{s1}\omega'_{s2} = 0 \tag{12-110}$$

for ω'_{p2}. Hence†

$$\omega'_{p2} = \frac{k}{2}(\omega'_{s2} - \omega'_{s1}) + \sqrt{\frac{k^2}{4}(\omega'_{s2} - \omega'_{s1})^2 + \omega'_{s1}\omega'_{s2}} \tag{12-111}$$

while

$$\omega'_{p1} = \frac{\omega'_{s2}\omega'_{s1}}{\omega'_{p2}} = \omega'_{p2} - k(\omega'_{s2} - \omega'_{s1}) \tag{12-112}$$

Next, from (12-104) and (12-105),

$$A = \frac{\omega_p}{\omega'_{p2} - \omega'_{p1}} = \frac{\omega_s}{\omega'_{s2} - \omega'_{s1}} \qquad \omega_1^2 = \omega'_{s1}\omega'_{s2} = \omega'_{p1}\omega'_{p2} \tag{12-113}$$

Finally, the bandpass-filter-element values can be found from Fig. 12-22*a* and *b*, as well as Eqs. (12-99) and (12-102).

Example 12-7 Design a bandpass filter satisfying the following specifications:

For 4.82 MHz $\leq f \leq$ 5.18 MHz $\quad \alpha \leq 0.2$ dB

for $f \leq$ 4.34 MHz and $f \geq$ 5.66 MHz $\quad \alpha \geq 36$ dB

Both terminations must be 150 Ω.

Since (calculating in megahertz)

$$f'_{p1}f'_{p2} = 24.9676 > f'_{s1}f'_{s2} = 24.5644$$

we have to readjust f'_{p1} to

$$\frac{f'_{s1}f'_{s2}}{f'_{p2}} \approx 4.74216 \text{ MHz}$$

By (12-108), the minimum value of the low-pass filter selectivity is

$$k = \frac{f'_{p2} - f'_{p1}}{f'_{s2} - f'_{s1}} \approx \frac{0.43784}{1.32} \approx 0.3317$$

† The solution containing the negative sign before the square root yields $-\omega'_{p1}$.

When an elliptic-filter prototype is chosen from Table 12-8, the filter with $\theta = 21°$ may be selected. This filter has a maximum passband reflection factor $\rho_{max} = 20$ percent, corresponding to

$$\alpha_p = -10 \log \frac{P_2}{P_{max}} = -10 \log \frac{P_{max} - P_r}{P_{max}}$$

$$\alpha_p = -10 \log (1 - \rho_{max}^2) \approx 0.17729 \text{ dB}$$

where Eqs. (6-16) to (6-20) have been utilized. Since for this filter $\alpha_p < 0.2$ dB, $\alpha_s = 36.14$ dB > 36 dB, and $k = 1/\Omega_s \approx 0.35837 > 0.3317$, it meets all requirements. The circuit diagram is shown in Fig. 12-23*a*. The element values are obtained from Table 12-8 as $C_1 = 1.1215$, $C_2 = 0.0925$, $L_2 = 1.0593$, with a normalization such that $\omega_p = 1$.

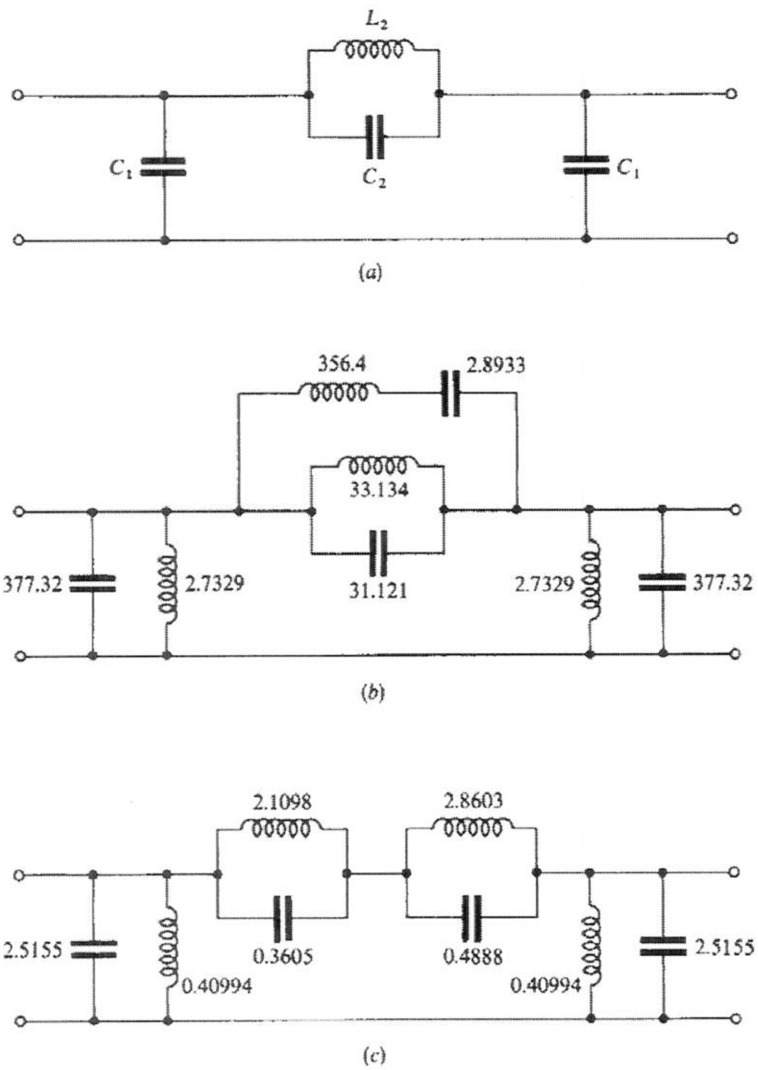

Figure 12-23 (*a*) Normalized low-pass elliptic filter, used as a prototype; (*b*) transformed-impedance-normalized-bandpass filter (element values in nanofarads and nanohenrys); (*c*) final bandpass filter (element values in nanofarads and microhenrys).

Keeping f'_{s_1} and f'_{s_2} unchanged and working in terms of f rather than ω, we see that Eq. (12-111) gives the readjusted passband limit

$$f'_{p_2} = \frac{k}{2}(f'_{s_2} - f'_{s_1}) + \sqrt{\frac{k^2}{4}(f'_{s_2} - f'_{s_1})^2 + f'_{s_1} f'_{s_2}} \approx 5.198365 \text{ MHz}$$

and from (12-112)

$$f'_{p_1} = \frac{f'_{s_1} f'_{s_2}}{f'_{p_2}} \approx 4.7254 \text{ MHz}$$

We note that the original specifications are met with some safety margin.

The transformation constants can be found from (12-113):

$$A = \frac{\omega_s}{\omega'_{s_2} - \omega'_{s_1}} = \frac{\Omega_s}{2\pi(f'_{s_2} - f'_{s_1})} \approx \frac{2.7904}{(2\pi)(1.32 \times 10^6)}$$

$$A \approx 0.336444 \times 10^{-6} \qquad \omega_1^2 = (2\pi)^2 f'_{s_1} f'_{s_2} \approx 969.76364 \times 10^{12}$$

Hence, by Fig. 12-22*b* and Eq. (12-102), C_1 becomes the parallel combination of a capacitance

$$C'_1 = AC_1 \approx 0.37732\ \mu\text{F}$$

and an inductance

$$L'_1 = \frac{1}{C'_1 \omega_1^2} \approx 2.7329 \text{ nH}$$

Similarly, L_2 is replaced by a series resonant circuit. The element values are, by (12-99),

$$L'_2 = AL_2 \approx 356.4 \text{ nH} \qquad C'_2 = \frac{1}{L'_2 \omega_1^2} \approx 2.8933 \text{ nF}$$

Finally, C_2 is replaced by a parallel tuned circuit with element values $AC_2 \approx 31.121$ nF and $1/\omega_1^2 AC_2 \approx 33.134$ nH (Fig. 12-23*b*).

The circuit of Fig. 12-23*b* is still impedance-normalized, since the prototype filter has 1-Ω terminations. Furthermore, the element values (although positive and thus theor-

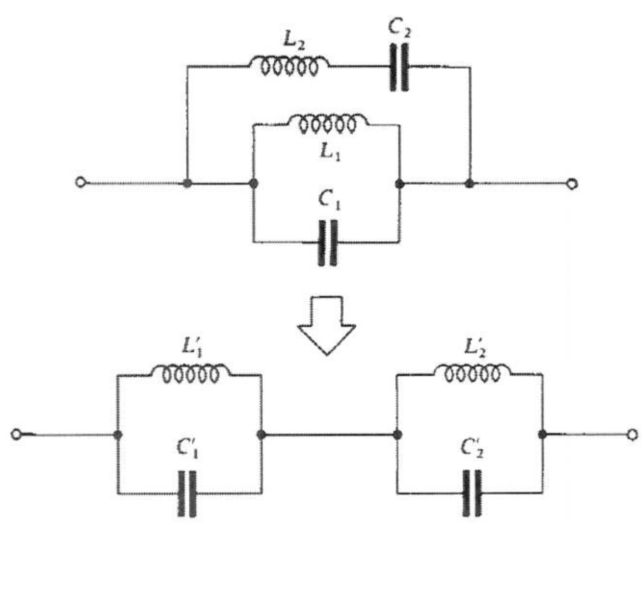

Figure 12-24 A network equivalence.

etically realizable) are too widely spread for easy practical construction; the ratios L'_2/L'_1 and C'_1/C'_2 are over 130.

It is known from experience that this phenomenon is often encountered for *narrow-band* bandpass filters, i.e., for filters where $\omega'_{p1} - \omega'_{p2} \ll \sqrt{\omega'_{p1}\omega'_{p2}}$, as is the case here. To remedy the situation, the circuit equivalence shown in Fig. 12-24 may be used. The circuits shown are equivalent if the following relations hold:

$$L'_1 = L_1 \frac{1-y}{2} \qquad C'_1 = C_2 x \frac{1-z}{2}$$
$$L'_2 = L_1 \frac{1+y}{2} \qquad C'_2 = C_2 x \frac{1+z}{2} \tag{12-114}$$

where

$$x \triangleq \left(1 + \frac{C_1}{C_2} + \frac{L_2}{L_1}\right)^2 - 4\frac{C_1}{C_2}\frac{L_2}{L_1}$$
$$y \triangleq \sqrt{1 - \frac{4L_2}{xL_1}} \qquad z \triangleq \sqrt{1 - \frac{4C_1}{xC_2}} \tag{12-115}$$

For the circuit of Fig. 12-23*b*, $C_1/C_2 = L_2/L_1$ and hence (12-115) gives

$$x = 44.0291 \qquad y = z = 0.15102$$

Hence, using (12-114) and denormalizing the impedance level, i.e., multiplying all inductances and dividing all capacitances by $R_0 = 150\ \Omega$, gives the element values indicated in Fig. 12-23*c*. The spread of element values is now less than 7.

Next, consider the frequency transformation

$$\omega = A\frac{\omega'}{\omega_1^2 - \omega'^2} \tag{12-116}$$

Proceeding as we did before with (12-97), we can readily derive the corresponding element transformations (Fig. 12-25*a* and *b*) and the ω-vs.-ω' curve (Fig. 12-25*c*). The latter makes it obvious that Eq. (12-116) transforms a low-pass filter into a bandstop one. Figure 12-25*d* illustrates (for a Chebyshev filter) the resulting mapping of the loss response.

Since the analysis of this transformation is a close parallel of that of the lowpass-to-bandpass transformation, the detailed calculations are left to the reader as an exercise (see Probs. 12-31 to 12-34).

A review of Eqs. (12-91), (12-97), and (12-116) reveals that each of these relations replaces ω by a *reactance function* $f(\omega')$ of ω'. This makes it possible to replace the immittances ωL_i and ωC_i of the lowpass prototype filter, one by one, by realizable reactances to obtain the final high-pass (or bandpass or bandstop) filter. Clearly this process can be generalized to more complicated reactance functions; however, the symmetry conditions which result become very complicated

---

Figure 12-25 (*a*) and (*b*) The transformation of low-pass prototype elements into bandstop filter impedances; (*c*) the transformation of the frequency variable; (*d*) the effect of the transformation on the loss response.

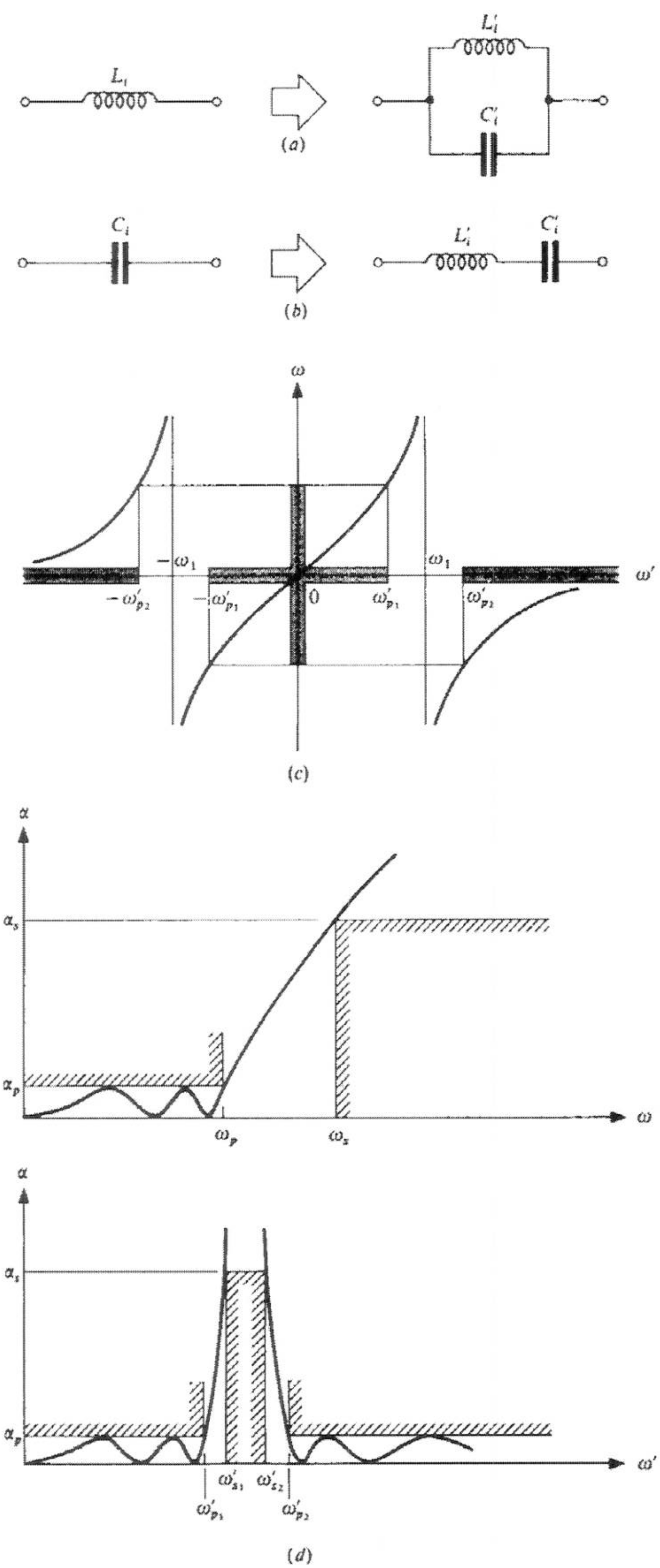
L_i
L_i'
C_i'
(a)
C_i
L_i'
C_i'
(b)
ω
$-\omega_1$
ω_1
ω'
$-\omega'_{p_2}$
$-\omega'_{p_1}$
0
ω'_{p_1}
ω'_{p_2}
(c)
α
α_s
α_p
ω_p
ω_s
ω
α
α_s
α_p
ω'_{s_1}
ω'_{s_2}
ω'
ω'_{p_1}
ω'_{p_2}
(d)